

Performance Evaluation of Waste Heat Recovery in a Charcoal Stove using a Thermo-Electric Module

Nnamdi Judges Ajah ^{1*}

¹ Nigerian Defence Academy, NIGERIA

*Corresponding Author: ajudges@gmail.com

Citation: Ajah, N. J. (2018). Performance Evaluation of Waste Heat Recovery in a Charcoal Stove using a Thermo-Electric Module. *European Journal of Sustainable Development Research*, 2(2), 25. <https://doi.org/10.20897/ejosdr/85187>

Published: March 13, 2018

ABSTRACT

Charcoal stoves have widespread use among the poorer households and outdoor food vendors in Nigeria. In order to improve the efficiency of charcoal stoves, various researches have tried integrating a thermoelectric module in the charcoal stove. The researches, however did not exploit the performance of the thermoelectric modules at different ambient temperatures. To evaluate the performance of thermoelectric integrated charcoal stoves in the sub-Saharan Africa, a self-powered, forced air induced thermoelectric charcoal stove experiment was carried out at five different ambient temperatures of 36°C, 33°C, 32°C, 30°C and 29°C and an average fuel hotbed temperature of 1023.75°C. The thermoelectric charcoal stove generated a maximum voltage of 5.25V at an ambient temperature of 29°C. The least maximum voltage was generated at the highest ambient temperature of 36°C. It was observed that the maximum voltage increased with decreasing ambient temperature, this could be attributed to the ambient air being used to cool the thermoelectric generator. Therefore, it could be said that the performance of a forced draft thermoelectric charcoal stove increases with decrease in ambient temperature.

Keywords: thermoelectric, charcoal, stove, sub-Saharan Africa

INTRODUCTION

Charcoal is widely accepted as fuel for cooking especially in Sub-Sahara Africa and other developing nations. Given that large numbers of people still use inefficient charcoal stoves (E+Carbon, 2009), it is necessary to design low-cost efficient charcoal burners.

For cooking stoves, the amount of the heat content of the charcoal transferred to the load/cooking vessel determines the efficiency. Equation 1 gives the formula for calculating the efficiency of the stove;

$$\eta_s = \frac{\text{Heat transferred to the load}}{\text{Heat content of fuel}} \quad (1)$$

Currently, a great deal of efforts have been put into making low-cost efficient charcoal burners. According to Toyola Energy Limited, their charcoal burner ToyolaCoalpot is 33% more fuel-efficient than traditional charcoal burners (E+Carbon, 2009). This is achieved by the introduction of a ceramic liner inside the combustion zone, which increases combustion efficiency and retains heat. The ceramic liner is said to have a potential to improve fuel efficiency by up to 50% (E+Carbon, 2009). Also, to achieve improved energy efficiency with low-cost, a prototype charcoal stove has been built using principles of combustion and heat transfer to improve stove efficiency (Milind, 2009).

A unique method of increasing efficiency of the charcoal burner is by recovering the waste heat; this can be done through the use of a thermoelectric module. The concept of thermoelectric generator (TEG) integrated stove research was first done by J.C Bass and Killander in 1996 (Killander and Bass, 1996). The main objective was to make the stove very affordable and efficient for rural people and others devoid of electricity.

Nuwayhid et al studied the possibility of using a proportion of the heat from 20-50kW wood stove, to provide a continuous 10-100W electric power supply (Nuwayhid et al., 2003). In a first prototype, they used a cheap Peltier module for their TE generator. The maximum power for a module was found to be very low (1W) mostly because of the limited temperature difference due to the maximum temperature supported by the module. It is also because of the geometry, which was optimized for cooling and not generating power. In addition, natural air was used to cool the cold-side of the module. In a subsequent prototype their TE generator used 1, 2 or 3 commercially available low-cost power generator modules (Nuwayhid and Hamade, 2005). The cold side of the TE modules was naturally cooled with the surrounding air. They got a maximum power of 4.2W for one thermoelectric module and they showed that the output per module decreased when the number of thermoelectric modules in the thermoelectric generator increased (Nuwayhid and Hamade, 2005). This is as a result of the decrease in temperature difference between opposite sides of the thermoelectric module.

Nuwayhid in one of the tests used heat pipes for the heat sink (Nuwayhid and Hamade, 2005). The maximum power obtained was about 3.4W. Lertsatitthanakorn replicated the same experiment with a commercial TE module made of bismuth telluride based materials to the stove's side wall, thereby creating a TE generator system that utilizes a proportion of the stove's waste heat, while also using heat pipes at the cold side to maintain a temperature difference across the module (Lertsatitthanakorn, 2007). The results show that the system generates a power output of approximately 2.4W when the temperature difference is 150°C. His economic analysis indicated that the payback period was very short.

At the ETHOS 2005 congress, Mastbergen and Wilson presented a prototype of a thermoelectric generator with a forced-air cooling for the cold side with a 1W fan (Mastbergen et al., 2005), 4W of net power was produced by the thermoelectric generator and it was able to power an array of high intensity LEDs.

Daniel Champier et al were able to produce 9.5W of electric power in a forced draft stove using bismuth telluride (Champier et al., 2011). Ice was used to maintain a temperature of under 100°C at the cold side and therefore a temperature difference across the module. They were able to show that the performance of the thermoelectric generator was influenced by the heat transfer through the modules and especially by the thermal contact resistances. The aluminum surface of the heat sinks used was reduced to a flatness of 25 micrometers (standard deviation of height). Mastbergen highlighted the role played by thermal contact resistances in thermoelectric generator performance (Mastbergen et al., 2005). According to him, the thermal resistances at the interfaces between the module and the heat sinks are also important to keep to a minimum, and recommended very flat surfaces of within 0.001". Daniel Champier et al suggested that a resistance of 500kPa was sufficient to minimize the contact resistance for the thermoelectric (Champier et al., 2011). In another experiment, Daniel Champier made use of four (4) TE modules in series and tried two different cooling systems (Champier et al., 2011):

1. A heat fins exchanger being placed on the cold side with a 10W air fan; and
2. A water tank directly put on the cold side of the TE module.

The amount of water contained in the tank applied a pressure of 10 kPa. A weight placed on rods above the fan applied the same pressure on the cell. By comparing the evolution of the temperature of the two cooling devices, it was learnt that for equivalent temperatures on the hot side, different temperatures on the cold side were reached. The cold-side temperature reached 117°C when the air fan was used, whereas, it was only 65°C with the use of ice; therefore, cooling with the air fan was not as efficient as with ice. In the experiment, a total power of about 7W was produced with a temperature difference of 160°C between the two sides of the generator. Measuring each cell independently to ascertain their individual performance, it was found that the maximum power reached by each module varied between 1.7W and 2.3W for a temperature difference between the sides of 160°C. It was also verified that the efficiency of a TE module is proportional to ΔT which is reasonable, as the output power is proportional to ΔT^2 and heat flux to ΔT . For a temperature difference of 60°C, the efficiency of a thermoelectric module is about 0.6% and the heat flow through the module is around 100W. However, a thermoelectric module efficiency of about 2% is obtained when computer simulation is done with a temperature difference of 200°C (Champier et al., 2011).

A commercially available biomass stove in the U.S., BioLite, uses a thermoelectric generator to create clean, efficient cooking with a forced-air draft fan (BioLite, 2015). Additionally, it has a 5W outlet powered by the TE generator that can be used to charge/power various electronic devices.

Rinalde et al were able to generate a maximum electrical power of 10W through the use of a heat pump, which certainly decreased the available output power (Rinalde et al., 2010). Their laboratory prototype used an electric

heater for the heat source and forced water cooling system to maintain a temperature difference across the thermoelectric module.

O'Shaughnessy et al used a single Seebeck optimized thermoelectric module with forced air cooling and heat pipes applied at the cold side of module to convert a small portion of heat from a stove to electricity (O'Shaughnessy et al., 2013). The electricity produced was used to charge a single 3.3V lithium-ion phosphate battery and drive a low power fan, as well as some other auxiliary features. The airflow produced by the fan was used in conjunction with a commercially available heat pipe heat sink to maintain an adequate temperature difference across the thermoelectric module. From experiments in the laboratory, a maximum TEG power output of 5.9W has been obtained. On average, 3Wh of energy was stored in a battery during a typical 1hr long burn. Three 1hr long burns produced sufficient energy to fully charge the battery.

After going through various literatures, it has been found that the voltage generated by the thermoelectric module using natural and forced air cooled induction at different operating temperatures has not yet been exploited, this study therefore aims to fill in the gap.

OBJECTIVES

The objectives of this research was to retrofit a conventional charcoal burner with a thermoelectric generator to recover heat. After which, data from the system will be obtained detailing the electromotive force generated by the thermoelectric generator at different operating temperatures of the burner, and evaluation of the voltage generated by the thermoelectric generator of the charcoal stove at different ambient temperatures

MATERIALS AND METHODS

Materials

A TEG1-127-2.0-1.3 thermoelectric module manufactured by EVERREDtronics was bought online from Amazon store. The hot and cold sides of the module were identified. A silicon-based adhesive thermal grease, HT-GY260, with thermal conductivity greater than 1W/m.K and thermal impedance less than 1.36°C-cm²/W was applied on the both surfaces of the thermoelectric module. This was done to obtain reasonable heat transfer and interfacing of the thermoelectric module with heat sinks. Two extruded aluminum heat-sinks of dimensions 28 x 28 x 20mm were obtained online from Amazon, and their top drilled to allow for insertion of type-J thermocouples. With thermal grease serving as the interfacing material, the thermoelectric module was placed in-between the two heat sinks to form the thermoelectric generator (TEG).

A low-permanence magnet DC driven fan of rated voltage 0.5-5 V and rpm of 3800 was placed at the fin side of the heat-sink attached to the cold-side of the thermoelectric module to force draft to cool the TEG. The electrical terminals of the fan were joined with the terminals of the thermoelectric module, so that the fan could be powered from the power generated from the module.

A charcoal stove was obtained from a local store in Ibadan, Oyo State. Its combustion section was an inverted truncated square pyramid of base side 7.8cm, top side of 22.1cm, and height of 16.1cm giving a volume of approximately 3870cm³. Charcoal was sourced locally from the market in Kaduna, Nigeria. The charcoal was used as fuel in the charcoal stove. The thermoelectric generator was placed in a cut-out section of the wall of the combustion chamber of the charcoal (see [Figure 1](#)).

Type-J thermocouples were placed in the holes drilled in each of the heat-sinks, and a voltage sensor was placed was connected in parallel to the electrical terminals of the thermoelectric module. The type-J thermocouples and voltage sensors were hard-wired to an Arduino micro-controller.

Experimental Method

The temperature of the ambient where the experimental rig was setup was recorded. The coupled thermoelectric generator was placed on the hot path of the combustion product. Type-J thermocouples were used to measure the temperature difference across the generator, while the voltage transducer is used to record the generated voltage. The micro-controller collects the various data every 10 seconds and logs the data unto a computer. The handheld digital multi-meter was used to take measurements of the current and recorded by hand.

The thermoelectric charcoal stove was run at five different ambient temperatures of 36°C, 33°C, 32°C, 30°C and 29°C with an average fuel hotbed temperature of 1023.75°C. [Figures 2](#) and [3](#) show the thermoelectric charcoal stove in operation with the data being collected on a computer. The data were saved as text files and analyzed using R programming language.



Figure 1. Thermoelectric generator placed in the charcoal stove

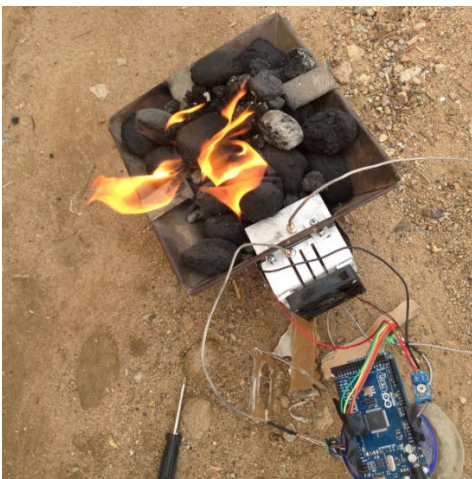


Figure 2. Experimental Rig

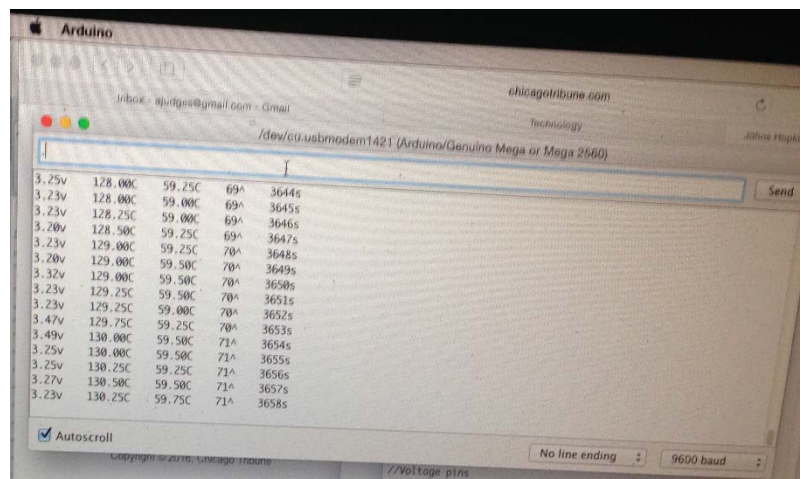


Figure 3. Data being displayed on the computer serial monitor

Calculating Efficiency of Cookstove

Firepower is the energy released by the burning fuel per unit time. Therefore, for any combustion phase, firepower can be calculated as follows (Chen et al., n.a):

$$\text{Fire power (W)} = \frac{(M_{ci} - M_{cf}) \times H_c}{\text{time}} \quad (2)$$

where:

P = power (W)

M_{ci} = initial mass of charcoal in the cook stove (g)

M_{cf} = final mass of charcoal in the cook stove (g)

H_c = energy content of charcoal (29000J/g)

Time = time of combustion phase (s)

Using the time it takes to boil water by a specified amount of the fuel, efficiency becomes the ratio of energy transferred to the water in the cooking pot to energy released by the burning fuel. Since the energy transferred to the water are in two phases – i.e. energy required to raise the temperature of water and energy required to evaporate the water – the efficiency will be calculated in two phases; hi-power phase (during temperature change of the water) and low-power phase (evaporation of the water). The following formulas which were gotten from literature (Chen et al., n.a), will be used in calculating efficiency,

During hi-power phase (conventional stove):

$$\text{Efficiency (\%)} = \frac{M_w \times C_w \times (T_f - T_i)}{(M_{ci} - M_{cf}) \times H_c} \quad (3)$$

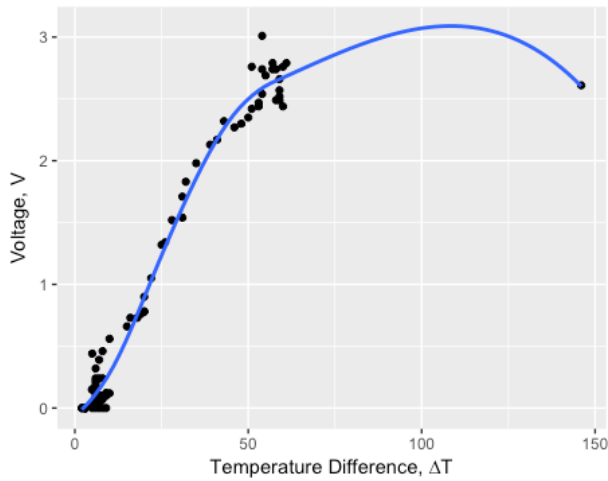


Figure 4. Voltage generated against temperature difference, at 36°C ambient temperature

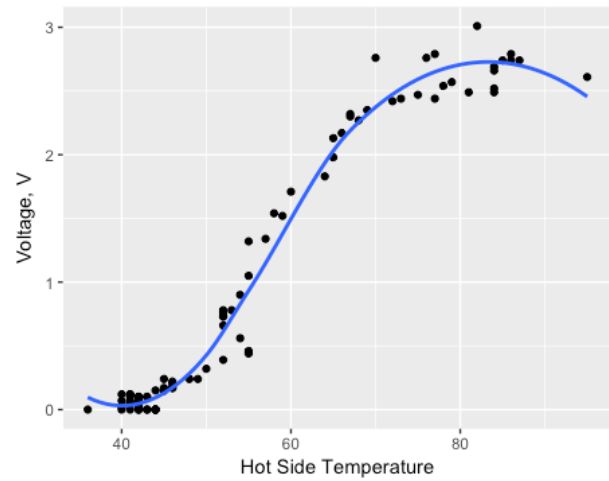


Figure 5. Voltage generated against hot side temperature, at 36°C ambient temperature

During hi-power phase (thermoelectric integrated stove):

$$Efficiency (\%) = \frac{M_w \times C_w \times (T_f - T_i) + (V_{av} I_{av} t)}{(M_{ci} - M_{cf}) \times H_c} \quad (4)$$

During low-power phase (conventional stove):

$$Efficiency (\%) = \frac{H_w \times (M_{wi} - M_{wf})}{(M_{ci} - M_{cf}) \times H_c} \quad (5)$$

During low-power phase (thermoelectric integrated stove):

$$Efficiency (\%) = \frac{H_w \times (M_{wi} - M_{wf}) + (V_{av} I_{av} t)}{(M_{ci} - M_{cf}) \times H_c} \quad (6)$$

where:

M_w = average water mass in the cook pot from pre-start to finish

C_w = heat capacity of water (4.184 J/g°C)

T_f = temperature of first boiling (°C)

T_i = initial temperature of the water in the pot (°C)

H_w = heat of vaporization of water (2260 J/g)

V_{av} = average voltage generated during operation

I_{av} = average current generated during operation

T = time

RESULTS AND DISCUSSION

The charcoal stove was operated at an average fuel hot-bed temperature of 1023.75°C and run at five different ambient temperatures of 29°C, 30°C, 32°C, 33°C and 36°C. Readings were taken every 10 seconds for a total of 15 minutes. Natural air-cooling was used until the voltage generated by the thermoelectric module reached 0.5 V after which it was able to power the fan to force draft to cool the TEG.

Case 1: At Ambient Temperature of 36°C

A maximum voltage of 3.01 V was achieved, and this occurred at a temperature difference of 54°C and a hot-side temperature of 136°C. The value of voltage increased linearly with the temperature difference before reaching its peak, after which it started forming a downward curve (Figure 4). The mean voltage generated was 0.9964 V and the median voltage value is 0.36 V. The mean temperature difference is $\Delta T_{mean} = 23.84^\circ\text{C}$, while the maximum temperature difference is 150°C with a corresponding hot side temperature of 241°C and voltage of 2.61 V. The graph of voltage generated against the hot side temperature is shown in Figure 5. Voltage increases linearly with increase in hot side temperature, after which it starts to form a downward curve. At a voltage of 0.5 V, where the powering of the fan by the TEG starts, gives a hot side temperature of 64°C and temperature difference of 10.

Table 1. Summary of parameters at 36°C ambient temperature

	Voltage	Hot side temp (T1)	Temperature difference, ΔT
Min.	0.000	45.00	2.00
1 st quartile	0.078	49.00	6.00
Median	0.355	57.50	9.00
Mean	0.996	79.41	23.84
3 rd quartile	2.293	112.25	45.25
Max.	3.010	241.00	146.00

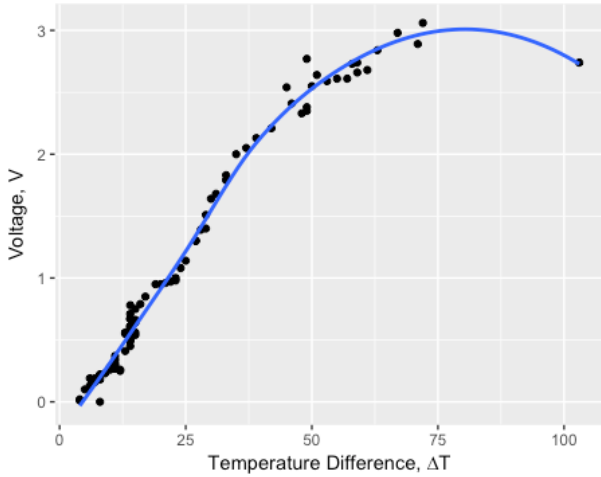


Figure 6. Voltage generated against temperature difference, at 33°C ambient temperature

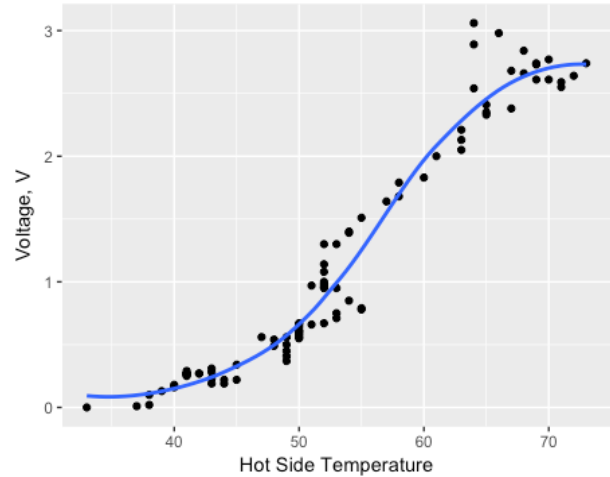


Figure 7. Voltage generated against hot side temperature, at 33°C ambient temperature

Table 2. Summary of parameters at 33°C ambient temperature

	Voltage	Hot side temp (T1)	Temperature difference, ΔT
Min.	0.000	41.00	4.00
1 st quartile	0.295	53.25	11.00
Median	0.730	67.50	15.00
Mean	1.146	78.83	25.81
3 rd quartile	2.038	98.25	36.50
Max.	3.060	176.00	103.00

Table 1 provides a summary of the parameters operating at 36°C ambient temperature. The data used can be seen at appendix A.1

Case 2: At Ambient Temperature of 33°C

Here, maximum voltage of 3 V was achieved at a temperature difference of 72°C and hot side temperature of 136°C. The voltage increased linearly up to 2.7 V before it started curving downwards **Figure 6**. The mean voltage obtained is 1.15 V with the median voltage value at 0.73 V. The mean temperature difference is $\Delta T_{\text{mean}}=25.81^\circ\text{C}$, while the maximum temperature difference ($\Delta T=103^\circ\text{C}$) (see **Figure 7**) occurred at a hot side temperature of 176°C and gave a voltage of 2.74 V. At the voltage of 0.5 V, where the fan starts to be powered, the hot side temperature and temperature difference were 63°C and 14°C respectively.

Table 2 provides a summary of the parameters operating at 33°C ambient temperature. The data used to generate the table can be found in appendix A.2

Case 3: At Ambient Temperature of 32°C

The voltage increased linearly to up to its peak 3.49 V at a temperature difference of 86°C (**Figure 8**). From **Figure 9** the peak voltage occurred at a hot side temperature of about 55°C. The mean voltage generated is 1.34 V and the median voltage is 1.15 V. The mean temperature difference is $\Delta T_{\text{mean}} = 29.04^\circ\text{C}$, while the maximum temperature difference obtained is 86°C, and the corresponding voltage and hot side temperature are 3.49 V and 141°C respectively. At the 0.5 V voltage point, the hot side temperature was 60°C and temperature difference of 17°C.

Table 3 provides a summary of the parameters operating at 32°C ambient temperature. The data used to generate the table can be found in appendix A.3

Case 4: At Ambient Temperature of 30°C

Voltage peaked at 4.36 V after increasing linearly. The maximum voltage occurred at a temperature difference of 89°C (**Figure 10**) and a hot side temperature of 150°C (**Figure 11**). The mean and median voltages are 1.94 V

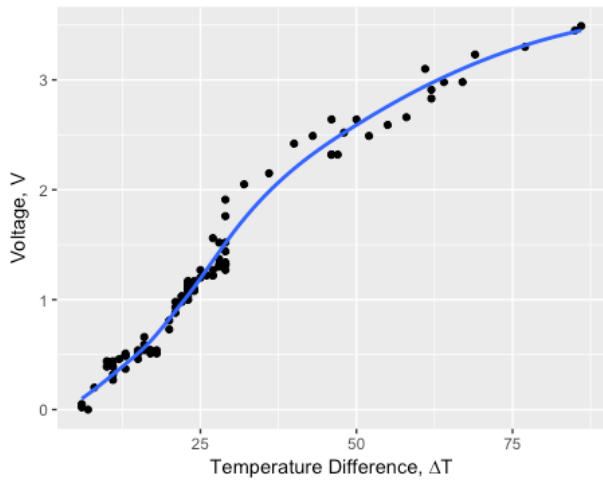


Figure 8. Voltage generated against temperature difference, at 32°C ambient temperature

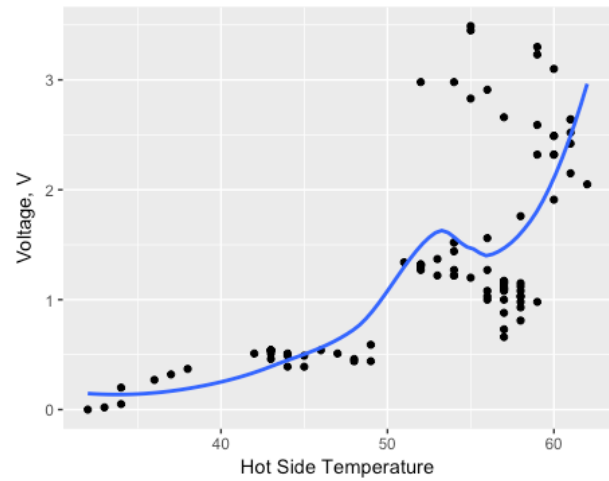


Figure 9. Voltage generated against hot side temperature, at 32°C ambient temperature

Table 3. Summary of parameters at 32°C ambient temperature

	Voltage	Hot side temp (T1)	Temperature difference, ΔT
Min.	0.000	39.00	6.00
1 st quartile	0.540	60.25	17.00
Median	1.150	80.00	24.00
Mean	1.343	81.62	29.04
3 rd quartile	1.873	89.00	29.00
Max.	3.490	141.00	86.00

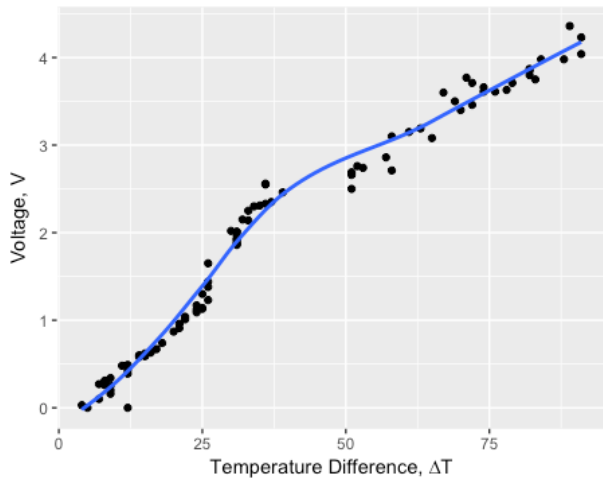


Figure 10. Voltage generated against temperature difference, at 30°C ambient temperature

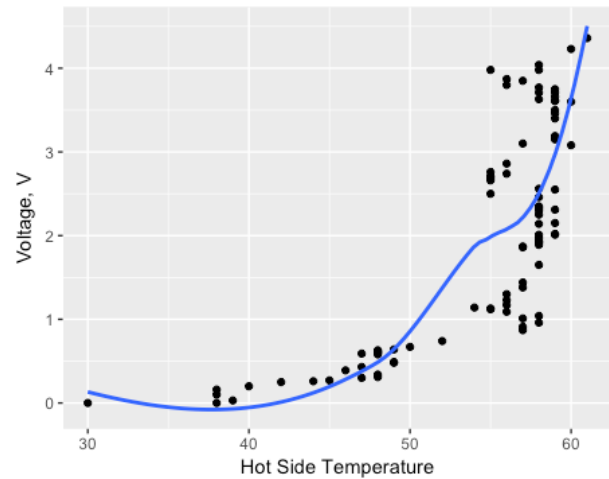


Figure 11. Voltage generated against hot side temperature, at 30°C ambient temperature

and 1.950 V respectively. The mean temperature difference is $\Delta T_{\text{mean}} = 38.47^\circ\text{C}$, while maximum temperature difference of 91°C was achieved with corresponding voltage and hot side temperature of 4.23 V and 151°C respectively. At the voltage point (0.5 V) of powering the fan, the temperature difference and hot side temperature were 12°C and 61°C respectively.

Table 4 provides a summary of the parameters operating at 30°C ambient temperature. The data used to generate the table can be found in appendix A.4

Case 5: At Ambient Temperature of 29°C

Voltage increased linearly with respect to temperature difference and peaked at 5.25 V with corresponding temperature difference of 92°C (**Figure 12**), and hot side temperature of 159°C (**Figure 13**). The mean and median voltages are 2.56 V and 2.788 V respectively. The mean temperature difference obtained is $\Delta T_{\text{mean}} = 48.13^\circ\text{C}$, while the maximum obtained temperature difference is 106°C , with corresponding voltage of 4.79 V and hot side temperature of 164°C . At the 0.5 V point where the thermoelectric starts to power the fan, the hot side temperature was 62°C and temperature difference of 7°C .

Table 4. Summary of parameters at 30°C ambient temperature

	Voltage	Hot side temp (T1)	Temperature difference, ΔT
Min.	0.000	42.00	4.00
1 st quartile	0.648	65.50	16.25
Median	1.950	89.00	31.00
Mean	1.944	92.64	38.47
3 rd quartile	3.095	118.75	60.25
Max.	4.360	151.00	91.00

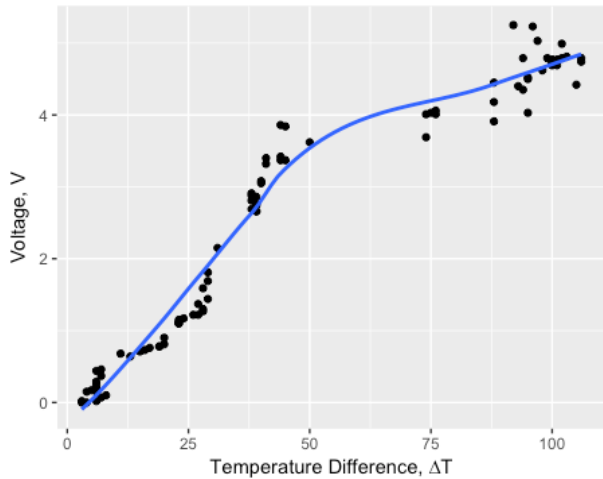


Figure 12. Voltage generated against temperature, at 29°C ambient temperature

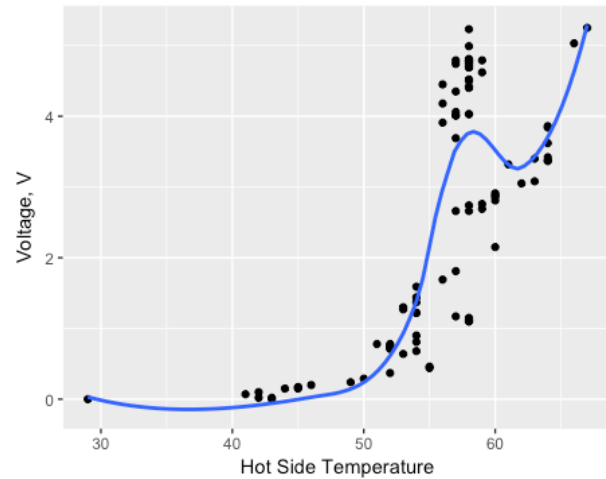


Figure 13. Voltage generated against hot side temperature, at 29°C ambient temperature

Table 5. Summary of parameters operating at 29°C ambient temperature

	Voltage	Hot side temp (T1)	Temperature difference, ΔT
Min.	0.000	45.00	3.00
1 st quartile	0.788	71.75	19.25
Median	2.785	98.00	39.00
Mean	2.560	103.78	48.13
3 rd quartile	4.308	149.50	91.00
Max.	5.250	164.00	106.00

Table 6. Power and efficiency values of the conventional and thermoelectric burner

	Conventional Burner	Thermoelectric burner
	Ambient temperature of 29°C	Ambient temperature of 29°C
Hi-power phase	Fire power (W)	2924W
	Efficiency (%)	20.24%
Low-power phase	Fire power (W)	656W
	Efficiency (%)	57.00%

Table 5 provides a summary of the parameters operating at 30°C ambient temperature. The data used to generate the table can be found in appendix A.5.

The graphs of voltage generated versus hot side temperature, T1, for ambient temperatures of 29°C, 30°C and 32°C follow a similar linear pattern, however for ambient temperatures of 33°C and 36°C, a downward curve begins to appear at about 60°C. Similarly graphs of voltage generated versus ΔT for ambient temperatures of 29°C, 30°C and 32°C have the same pattern, while ambient temperatures of 33°C and 36°C take a different pattern. It can be seen that voltage generally increases with an increase in the hot side temperature for all ambient temperatures, with the highest voltage recordings being 5.25 V at an ambient temperature of 29°C. It is observed that from an ambient temperature of 36°C, each subsequent lower ambient temperature recorded a higher and maximum voltage values. Likewise, the mean voltage values increased with lower ambient temperature. Explanation for this phenomenon could come from the fact that since ambient air is used to cool the thermoelectric generator enabling temperature difference across the module, the lower the ambient temperature the more effective temperature difference is achieved across the module. This is substantiated from the data on temperature difference, where the mean temperature difference across the module is higher with decreasing ambient temperature. The mean temperature difference for 29°C ambient temperature, which had the highest maximum and mean voltage readings, is $\Delta T_{\text{mean}} = 48.13^\circ\text{C}$; while for 36°C ambient temperature which had the lowest maximum and mean voltage readings, is $\Delta T_{\text{mean}} = 23.84^\circ\text{C}$.

Calculating and Comparing the Efficiency of the Thermoelectric Charcoal Stove with a Conventional Charcoal Stove of Similar Size at the Same Ambient Temperature of 29°C.

From Equations 2 – 6,
High-power phase Firepower

$$\text{Fire power (W)} = \frac{(M_{ci} - M_{cf}) \times H_c}{\text{time}} = \frac{138g \times 29000J/g}{17 \text{ min} \times 60s/\text{min}} = 2924W$$

Low-power phase Firepower,

$$\text{Fire power (W)} = \frac{(M_{ci} - M_{cf}) \times H_c}{\text{time}} = \frac{19g \times 29000J/g}{14 \text{ min} \times 60s/\text{min}} = 656 W$$

Efficiency for Conventional Charcoal Stove of Volume Capacity 3870 cm³ at 29°C Ambient Temperature

High-power phase:

$$\text{Efficiency (\%)} = \frac{M_w \times C_w \times (T_f - T_i)}{(M_{ci} - M_{cf}) \times H_c} = \frac{2652g \times 4.184J/g^\circ C \times (100 - 27)^\circ C}{138g \times 29000J/g} = 20.24\%$$

Low-power phase:

$$\text{Efficiency (\%)} = \frac{H_w \times (M_{wi} - M_{wf})}{(M_{ci} - M_{cf}) \times H_c} = \frac{2260J/g \times 139g}{19g \times 29000J/g} = 57.00\%$$

Efficiency for Thermoelectric Charcoal Stove of Volume Capacity 3870 cm³ at 29°C Ambient Temperature

High-power phase:

$$\begin{aligned} \text{Efficiency (\%)} &= \frac{M_w \times C_w \times (T_f - T_i) + (I_{av} V_{av} t)}{(M_{ci} - M_{cf}) \times H_c} \\ &= \frac{2652g \times \frac{4.184J}{g}^\circ C \times (100 - 27)^\circ C + (2.56 * 0.43) * (17 * 60)}{138g \times 29000J/g} = 20.27\% \end{aligned}$$

Low-power phase:

$$\begin{aligned} \text{Efficiency (\%)} &= \frac{H_w \times (M_{wi} - M_{wf}) + (V_{av} I_{av} t)}{(M_{ci} - M_{cf}) \times H_c} \\ &= \frac{2260J/g \times 139g + (2.56 * 1) * (17 * 60)}{19g \times 29000J/g} = 57.49\% \end{aligned}$$

Tabulating the result of the computations,

Table 6 shows the various power and efficiency values of the conventional and thermoelectric burner at 29°C ambient temperature. The thermoelectric burner is seen to have a slightly higher efficiency than the conventional charcoal burner.

CONCLUSION

The development of a conventional charcoal burner with a thermoelectric generator attached to it has been achieved and tested under real-life cooking conditions in sub-Saharan Africa. The e.m.f generated by the thermoelectric charcoal stove generally increases with increase in the hot side temperature of the thermoelectric module. When using ambient air to cool the thermoelectric module, the performance of the thermoelectric module increases with a decrease in ambient temperature. This is as a result of the lower ambient temperature enabling a higher temperature difference across the thermoelectric generator.

While the improved efficiency of a thermoelectric charcoal stove over a conventional charcoal stove is not so higher, the electrical energy from it can be put to good use, such as charging batteries and powering LEDs

REFERENCES

BioLite. (2015). BioLite CampStove. Available at: <http://www.biolitestove.com/products/biolite-campstove>

Chen, Y., Pew, D., Abbott D. (n.a.). Cook Stove Efficiency, Health and Environmental Impacts: Biomass Lab Report. Available at: <http://stoves.bioenergylists.org/files/er120-1biomass.pdf>

Champier, D., Bedecarrats, J. P., Kousksou, T., Rivaletto, M., Strub, F. and Pignolet, P. (2011). Study of a Thermoelectric Generator incorporated in a multifunction wood stove. *Energy Elsevier*, 36, 3, 1518.

E+Carbon. (2009). Improved Household Charcoal Stoves in Ghana, London. Available at: <http://cleancookstoves.org/binary-data/RESOURCE/file/000/000/108-1.pdf>

Killander, A. and Bass, J. C. (1996). A stove-top generator for cold areas. In: *Proceedings of the 15th International Conference on Thermoelectrics*, New York. <https://doi.org/10.1109/ICT.1996.553511>

Lertsatitthanakorn, C. (2007). Electrical performance analysis and economic evaluation of combined biomass cook stove thermoelectric (BITE) generator. *Bioresource Technology*, 98, 1670-1674. <https://doi.org/10.1016/j.biortech.2006.05.048>

Mastbergen, D., Wilson, B. and Joshi, S. (2005). Producing Light from Stoves using a Thermoelectric Generator. In: *ETHOS International Stove Research Conference*, Seattle, Washington, 15-27.

Milind, P. K. (2009). Experimental study for improving energy efficiency of charcoal stove. *Journal of Scientific and Industrial Research*, 68, 412-416.

Nuwayhid, R. Y., Rowe, D. M and Min, G. (2003). Low Cost Stove-Top Thermoelectric Generator for Regions with Unreliable Electricity Supply. *Renewable Energy*, 28, 205-222. [https://doi.org/10.1016/S0960-1481\(02\)00024-1](https://doi.org/10.1016/S0960-1481(02)00024-1)

Nuwayhid, R. Y. and Hamade, R. (2005). Design and testing of a locally made loop-type thermosiphonic heat sink for stove-top thermoelectric generator. *Renewable Energy*, 30, 1101-1116. <https://doi.org/10.1016/j.renene.2004.09.008>

O’Shaughnessy, S. M., Deasy, M. J., Kinsella, C. E., Doyle, J. V. and Robinson, A. J. (2013). Small scale electricity generation from a portable biomass cookstove: Prototype design and preliminary results. *Applied Energy*, 12, no. C, 374-385. <https://doi.org/10.1016/j.apenergy.2012.07.032>

Rinalde, G. F., Juanico, L. G., Tagliavore, E., Gortari, S. and Molina S. G. (2010). Development of thermoelectric generators for electrification of isolated rural homes. *International Journal of Hydrogen Energy*, 35(11), 5818-5822. <https://doi.org/10.1016/j.ijhydene.2010.02.093>

APPENDIX A

Table A.1. Data at ambient temperature of 36°C and average fuel hotbed temperature of 1023.75°C

Time (sec)	Voltage	T1	T2	T1-T2
10	0	45	36	9
20	0	45	42	2
30	0	45	43	2
30	0	46	43	3
40	0	46	44	3
50	0	47	44	3
60	0	47	44	3
70	0	47	44	3
80	0	47	44	3
90	0	48	42	5
100	0	48	42	6
110	0	48	40	8
120	0	48	41	7
130	0.02	47	40	7
140	0.02	48	42	6
150	0.02	47	42	6
160	0.02	48	42	5
170	0.05	47	41	6
180	0.05	47	41	6
190	0.05	47	41	6
200	0.07	48	41	7
210	0.07	48	40	8

220	0.07	48	42	7
230	0.07	49	42	7
240	0.1	49	42	7
250	0.1	49	43	6
260	0.1	49	43	7
270	0.1	50	42	8
280	0.1	50	42	8
290	0.1	50	41	9
300	0.12	49	41	9
310	0.12	50	41	9
320	0.12	50	40	10
330	0.15	50	45	5
340	0.15	50	45	5
350	0.15	50	45	5
360	0.15	50	44	6
370	0.17	50	45	6
380	0.17	51	46	6
390	0.17	52	46	6
400	0.2	52	46	6
410	0.22	52	46	6
420	0.24	52	45	8
430	0.24	54	48	6
440	0.24	55	49	7
450	0.32	56	50	6
460	0.39	59	52	7
470	0.44	60	55	5
480	0.46	63	55	8
490	0.56	64	54	10
500	0.66	66	52	15
510	0.73	68	52	16
520	0.73	70	52	18
530	0.76	71	52	19
540	0.78	72	52	20
550	0.78	73	53	20
560	0.9	75	54	20
570	1.05	77	55	22
580	1.32	80	55	25
590	1.34	83	57	26
600	1.52	87	59	28
610	1.54	89	58	31
620	1.71	91	60	31
630	1.83	95	64	32
640	1.98	100	65	35
650	2.13	104	65	39
660	2.17	107	66	41
670	2.32	110	67	43
680	2.27	113	68	46
690	2.3	115	67	48
700	2.35	119	69	50
710	2.76	122	70	51
720	2.42	122	72	51
730	2.44	126	73	53
740	2.47	128	75	53
750	2.54	132	78	54
760	3.01	136	82	54
770	2.69	140	84	55
780	2.74	141	87	54
790	2.79	143	86	57
800	2.74	143	85	58
810	2.66	143	84	59
820	2.74	143	86	57
830	2.61	241	95	146
840	2.49	141	84	58
850	2.52	142	84	59

860	2.49	140	81	59
870	2.57	139	79	59
880	2.79	137	77	61
890	2.44	137	77	60
900	2.76	136	76	60

Table A.2. Data at ambient temperature of 33°C and average fuel hot-bed temperature of 1023.75°C.

Time (sec)	Voltage	T1	T2	T1-T2
10	0.00	41	33	8
20	0.01	41	37	4
30	0.02	42	38	4
30	0.10	43	38	5
40	0.13	46	39	6
50	0.16	47	40	7
60	0.18	48	40	8
70	0.19	50	44	6
80	0.19	50	43	7
90	0.22	52	44	8
100	0.22	53	45	8
110	0.23	53	43	9
120	0.25	53	41	12
130	0.26	52	41	12
140	0.27	52	41	11
150	0.27	53	41	11
160	0.27	53	42	11
170	0.29	52	41	11
180	0.27	52	41	10
190	0.26	51	41	10
200	0.27	51	41	10
210	0.27	51	41	10
220	0.27	52	42	10
230	0.28	53	43	10
240	0.31	54	43	11
250	0.34	56	45	11
260	0.37	60	49	11
270	0.41	62	49	13
280	0.45	63	49	14
290	0.50	63	49	14
300	0.49	62	48	14
310	0.56	63	47	15
320	0.54	64	48	15
330	0.55	63	50	13
340	0.56	63	49	13
350	0.56	64	50	14
360	0.58	64	50	14
370	0.59	64	50	14
380	0.61	64	50	14
390	0.61	64	50	14
400	0.67	64	50	14
410	0.64	65	50	15
420	0.66	65	50	15
430	0.66	66	51	15
440	0.67	67	52	14
450	0.71	67	53	14
460	0.75	68	53	15
470	0.78	69	55	14
480	0.79	70	55	16
490	0.85	71	54	17
500	0.95	72	53	19
510	0.95	72	52	20
520	0.96	73	52	21
530	0.97	74	51	22
540	0.98	74	52	23
550	1.00	75	52	23
560	1.08	76	52	24
570	1.14	77	52	25
580	1.30	79	52	27

590	1.30	80	53	27
600	1.39	82	54	28
610	1.40	83	54	29
620	1.51	84	55	29
630	1.64	87	57	30
640	1.68	90	58	31
650	1.79	91	58	33
660	1.83	93	60	33
670	2.00	96	61	35
680	2.05	99	63	37
690	2.13	102	63	39
700	2.21	106	63	42
710	2.54	109	64	45
720	2.41	110	65	46
730	2.33	113	65	48
740	2.35	114	65	49
750	2.38	116	67	49
760	2.77	119	70	49
770	2.55	122	71	50
780	2.64	123	72	51
790	2.59	125	71	53
800	2.61	126	70	55
810	2.61	126	69	57
820	2.73	127	69	58
830	2.74	176	73	103
840	2.68	128	67	61
850	2.66	127	68	59
860	2.74	128	69	59
870	2.84	131	68	63
880	2.98	134	66	67
890	2.89	135	64	71
900	3.06	136	64	72

Table A.3. Data at ambient temperature of 32°C and average fuel hot-bed temperature of 1023.75°C.

Time (sec)	Voltage	T1	T2	T1-T2
10	0.00	39	32	7
20	0.02	40	33	6
30	0.05	41	34	6
30	0.20	43	34	8
40	0.27	47	36	11
50	0.32	48	37	11
60	0.37	51	38	13
70	0.39	55	45	10
80	0.39	56	44	11
90	0.44	59	48	10
100	0.44	60	49	11
110	0.46	60	48	12
120	0.51	60	42	18
130	0.51	60	43	17
140	0.54	59	43	17
150	0.54	60	43	17
160	0.54	60	43	18
170	0.54	59	43	16
180	0.51	59	44	15
190	0.46	57	43	15
200	0.49	57	44	13
210	0.49	57	44	13
220	0.49	58	45	13
230	0.51	60	47	13
240	0.54	61	46	15
250	0.59	65	49	16
260	0.66	74	57	16
270	0.73	76	57	20
280	0.81	78	58	20
290	0.93	79	58	21
300	0.88	78	57	21
310	1.03	78	56	22
320	0.98	80	59	21

330	0.98	80	58	22
340	1.00	79	56	23
350	1.00	80	57	23
360	1.03	80	58	23
370	1.03	80	58	22
380	1.08	80	58	23
390	1.08	80	57	23
400	1.17	79	57	23
410	1.08	80	56	24
420	1.10	80	57	23
430	1.10	81	57	24
440	1.12	81	58	23
450	1.12	81	57	23
460	1.15	80	58	23
470	1.15	81	57	24
480	1.15	81	57	24
490	1.17	80	57	24
500	1.27	81	56	25
510	1.20	80	55	25
520	1.22	80	54	26
530	1.22	80	53	27
540	1.22	80	54	27
550	1.27	80	54	27
560	1.30	80	52	28
570	1.27	81	52	29
580	1.34	81	51	29
590	1.32	81	52	29
600	1.32	81	52	29
610	1.32	80	52	28
620	1.37	80	53	28
630	1.52	82	54	29
640	1.44	83	54	29
650	1.52	83	54	28
660	1.56	83	56	27
670	1.76	86	58	29
680	1.91	90	60	29
690	2.05	93	62	32
700	2.15	97	61	36
710	2.42	101	61	40
720	2.49	103	60	43
730	2.32	106	60	46
740	2.32	106	59	47
750	2.32	106	60	46
760	2.64	107	61	46
770	2.52	109	61	48
780	2.64	110	61	50
790	2.49	112	60	52
800	2.59	113	59	55
810	2.66	115	57	58
820	2.83	116	55	62
830	2.98	118	54	64
840	2.98	119	52	67
850	2.91	117	56	62
860	3.10	121	60	61
870	3.23	128	59	69
880	3.30	136	59	77
890	3.45	140	55	85
900	3.49	141	55	86

Table A.4. Data at ambient temperature of 30°C and average fuel hot-bed temperature of 1023.75°C.

Time (sec)	Voltage	T1	T2	T1-T2
10	0.00	42	30	12
20	0.00	43	38	5
30	0.03	43	39	4
30	0.10	45	38	7
40	0.16	47	38	9
50	0.20	49	40	9
60	0.25	50	42	9

70	0.27	52	45	7
80	0.26	53	44	8
90	0.30	55	47	8
100	0.31	56	48	8
110	0.34	57	48	9
120	0.39	58	46	12
130	0.43	59	47	12
140	0.48	60	49	11
150	0.49	61	49	12
160	0.60	63	48	14
170	0.58	62	48	14
180	0.60	63	48	15
190	0.59	62	47	15
200	0.62	63	48	15
210	0.62	63	48	15
220	0.63	64	48	16
230	0.64	65	49	16
240	0.67	67	50	17
250	0.74	70	52	18
260	0.87	77	57	20
270	0.91	79	57	21
280	0.96	79	58	21
290	1.04	80	58	22
300	1.01	79	57	22
310	1.12	79	55	24
320	1.09	80	56	24
330	1.17	80	56	24
340	1.14	80	54	25
350	1.13	80	55	25
360	1.30	81	56	25
370	1.23	82	56	26
380	1.38	83	57	26
390	1.44	83	57	26
400	1.65	85	58	26
410	1.86	88	57	31
420	1.87	88	57	31
430	1.89	89	58	31
440	1.92	89	58	31
450	1.93	89	58	31
460	2.02	89	59	30
470	2.01	89	59	31
480	1.97	90	58	31
490	2.01	90	58	31
500	2.15	91	59	32
510	2.25	91	58	33
520	2.14	91	58	33
530	2.30	92	58	34
540	2.31	94	59	35
550	2.55	94	59	36
560	2.33	94	58	36
570	2.56	95	58	36
580	2.35	95	58	37
590	2.46	97	58	39
600	2.50	106	55	51
610	2.66	106	55	51
620	2.69	106	55	51
630	2.76	107	55	52
640	2.74	108	56	53
650	2.71	113	55	58
660	2.86	113	56	57
670	3.10	115	57	58
680	3.15	120	59	61
690	3.19	122	59	63

700	3.08	125	60	65
710	3.60	127	60	67
720	3.50	128	59	69
730	3.40	130	59	70
740	3.77	130	58	71
750	3.46	131	59	72
760	3.71	132	59	72
770	3.61	133	59	74
780	3.66	134	59	74
790	3.61	135	59	76
800	3.63	136	58	78
810	3.71	137	58	79
820	3.80	138	56	82
830	3.87	138	56	82
840	3.98	139	55	84
850	3.85	139	57	82
860	3.75	142	59	83
870	3.98	146	58	88
880	4.04	150	58	91
890	4.23	151	60	91
900	4.36	150	61	89

Table A.5. Data at ambient temperature of 29°C and average fuel hot-bed temperature of 1023.75°C.

Time (sec)	Voltage	T1	T2	T1-T2
10	0.00	45	29	3
20	0.00	46	43	4
30	0.02	46	43	3
30	0.02	47	42	6
40	0.07	48	41	7
50	0.10	49	42	8
60	0.15	49	45	4
70	0.17	50	45	5
80	0.15	50	44	6
90	0.17	51	45	6
100	0.20	52	46	6
110	0.24	54	49	6
120	0.29	56	50	6
130	0.37	58	52	7
140	0.44	61	55	6
150	0.46	62	55	7
160	0.68	65	54	11
170	0.68	65	54	11
180	0.64	66	53	13
190	0.71	67	52	15
200	0.73	68	52	16
210	0.76	69	52	17
220	0.78	70	51	19
230	0.78	71	52	19
240	0.81	74	54	20
250	0.90	74	54	20
260	1.10	81	58	23
270	1.10	81	58	23
280	1.12	81	58	23
290	1.17	81	57	24
300	1.15	81	58	23
310	1.22	80	54	26
320	1.22	81	54	27
330	1.37	80	54	27
340	1.30	81	53	28
350	1.27	81	53	28
360	1.59	82	54	28
370	1.44	83	54	29
380	1.69	85	56	29
390	1.81	85	57	29
400	2.15	91	60	31
410	2.66	96	57	39
420	2.66	97	58	39

430	2.69	97	59	38
440	2.74	97	58	39
450	2.76	98	59	39
460	2.91	98	60	38
470	2.88	98	60	38
480	2.81	98	60	38
490	2.86	99	60	39
500	3.05	102	62	40
510	3.32	102	61	41
520	3.08	102	63	40
530	3.40	103	63	41
540	3.42	108	64	44
550	3.84	108	64	45
560	3.37	107	64	44
570	3.86	108	64	44
580	3.37	109	64	45
590	3.62	114	64	50
600	3.69	131	57	74
610	4.01	131	57	74
620	4.03	132	58	75
630	4.01	133	57	76
640	4.06	133	57	76
650	3.91	144	56	88
660	4.18	144	56	88
670	4.45	145	56	88
680	4.40	151	58	93
690	4.35	151	57	94
700	4.03	153	58	95
710	4.79	153	59	94
720	4.52	153	58	95
730	4.50	154	58	95
740	5.23	154	58	96
750	4.62	157	59	98
760	4.79	157	58	99
770	4.72	158	58	100
780	4.69	158	58	100
790	4.74	158	58	100
800	4.69	159	58	101
810	4.77	159	58	101
820	4.79	159	57	102
830	4.77	158	58	100
840	4.99	160	58	102
850	4.81	160	58	103
860	4.42	163	58	105
870	4.74	163	57	106
880	4.79	164	58	106
890	5.03	163	66	97
900	5.25	159	67	92